73rd International Astronautical Congress (IAC), Paris, France, 18-22 September 2022.

IAC-22,C1,IP,19,x73745

Modelling and simulation of an on-orbit experiment for testing a novel engine technology

Martina Rusconi[a]*, Giacomo Borelli[b], Vincenzo Tirella[c], Camilla Colombo[d], Giovanni Consolati[e]

[a] *Department of Aerospace Science and Technology, Politecnico di Milano, Via La Masa 34, 20256, Milano, Italy,* martina.rusconi@polimi.it
[b] *Department of Aerospace Science and Technology, Politecnico di Milano, Via La Masa 34, 20256, Milano, Italy,* giacomo.borelli@polimi.it
[c] *Genergo S.r.l., via Cadorna 5, 22100, Como, Italy*
vincenzo.tirella@gmail.com
[d] *Department of Aerospace Science and Technology, Politecnico di Milano, Via La Masa 34, 20256, Milano, Italy,* camilla.colombo@polimi.it
[e] *Department of Aerospace Science and Technology, Politecnico di Milano, Via La Masa 34, 20256, Milano, Italy,* giovanni.consolati@polimi.it
* Corresponding Author

Abstract

The paper describes the design and modelling of an on-orbit mission experiment for testing a novel engine technology in Space. The goal is to assess the novel engine thrust profile through an on-orbit reverse engineering approach. The simulation tool developed at Politecnico di Milano is initially designed to propagate the free attitude dynamics of a spacecraft under the effect of main environment perturbations. Each element of the simulator is validated, prior to the on-orbit experiment, by matching orbit and attitude data from a previous similar mission of the ION spacecraft CubeSat carrier. The novel engine technology is located in one of the ION CubeSat slots and activated in orbit. The simulation tool is adapted to simulate the on-orbit experiments given the information on the attitude engine action and the mass and structure properties of the satellite. The preliminary analysis performed on the in-flight results of the tests highlighted the need of the development of smoothing techniques prior applying the reverse engineering approach. Some uncertain parameters, such as the carrier spacecraft inertias, showed a significant influence on the simulator's performance. Different methods have been applied to characterise the unmodelled dynamics and approximations' effects on the results. Future updates and corrections to the simulator are suggested to deal with the observed problems and improve the detection of the engine thrust magnitude. No end-results of the on-orbit mission experiment are presented in this paper, since the in-space operations are still on-going.

Keywords: reverse engineering, novel engine, attitude modelling, attitude simulation

Nomenclature

A_{cross}	Cross sectional area	m^2
A_i	Area of -i^{th} external surface	m^2
$\boldsymbol{a_{CG}}$	Orbital acceleration of the COG	m/s^2
$\boldsymbol{a}_{perturbations}$	Perturbing acceleration	m/s^2
$\boldsymbol{a_{xx}}$	Perturbing acceleration due to xx phenomenon	m/s^2
$\boldsymbol{b}$	Geomagnetic field	T
$C_{diff/spec_i}$	Specular/diffuse reflection coefficient of -i^{th} external surface	
C_d	Drag coefficient	
C_r	Reflectivity coefficient	
$\boldsymbol{F}_{i_{drag/srp}}$	Force acting on -i^{th} external surface	N
$\boldsymbol{g}_{Earth}$	Earth gravity acceleration	m/s^2
$\boldsymbol{J}$	Inertia tensor	kgm^2
$\boldsymbol{m}$	Satellite residual magnetic dipole	Am^2
μ_{Earth}	Earth gravitational parameter	m^3/s^2
$\boldsymbol{\hat{n}_i}$	Normal to -i^{th} external surface	
p_{srp}	SRP pressure	N/m^2
$\boldsymbol{q}$	Quaternion	
$\boldsymbol{r}$	Orbital position vector	m
ρ	Air density	kg/m^3
$\boldsymbol{T}_{d_{xx}}$	Perturbing torque caused by xx phenomenon	Nm
$\boldsymbol{T}_d$	Vector of environment perturbing torques	Nm
$\boldsymbol{T}_u$	Vector of external torques	Nm
t_i	Time at step i	s
$\boldsymbol{v}$	Orbital velocity vector	m/s
$\boldsymbol{v}_{rel}$	Relative velocity	m/s
$\boldsymbol{\omega}$	Angular velocity vector	$°/s$

$\boldsymbol{x}$	Vector
x	Magnitude
$\hat{\boldsymbol{x}}$	Unit vector
$\boldsymbol{X}$	Matrix

Acronyms/Abbreviations

COG	Centre Of Gravity
LEO	Low Earth Orbit
IR	InfraRed
SRP	Solar Radiation Pressure
GG	Gravity Gradient
EXP1	Torque-free telemetry of a previous mission used for preliminary validation
EXP2	Torque-free telemetry of the engine mission
EXP3	Telemetry of one set of tests of the engine mission
ECI	Earth Centred Inertial

1. Introduction

A novel engine technology has been developed by Genergo as a valuable propulsion mean for Space application. The company is interested in assessing engine operation and characterise its performance in Space. On-orbit experiments of a first-generation engine are currently being executed, with the aim of obtaining the data needed to parametrise and optimise a first-generation engine, as well as verifying some basic construction designs. Further technical developments will be configured and tested in future missions. The propulsor is carried by a satellite as part of its payload and fires for a limited amount of time during each test. Telemetry data of the spacecraft are recorded, they need to be analysed to investigate and detect the thrust action of the novel engine. A digital simulator of the satellite orbit and attitude motion is under development. Comparing in-flight data and the predicted motion of the simulated satellite the goal is to assess the operability of the engine and to retrieve its thrust profile. The simulator is also exploited for mission experiment design. The predicted outcome of the tests and the real-time results from in-flight data support the definition of operations of the mission.

The design of a digital reproduction of a real spacecraft requires time, multiple fields of competence and develops in successive phases. The work described in the paper refers to the first iteration of the design. A preliminary version of an orbit and attitude simulator has been built to have a ready instrument for data analysis during the current mission of the engine. It has been designed specifically to fulfil the goals introduced and was limited by the application's requirements and constraints. The simulator can be considered as the baseline work for a future digital twin of the physical spacecraft. Model-based design is acquiring large popularity in the Space field. A digital reproduction of a physical system helps its management and maintenance during the whole life cycle [1]. Performance and applications are widened by continuous exchange of data between the digital reproduction and the physical system [2]. Spacecraft autonomy and intelligence would increase [1]. The module of the simulator propagating orbit and attitude dynamics, with real telemetry data processed in the loop, would be a valuable tool for mission analysis and satellite safety monitoring. Given the physical satellite model, its long-term interaction with the environment may be predicted with high-fidelity simulations; motion evolution during on-orbit experiments would be investigated and the in-flight operations would be consequently defined. The effect of any manoeuvre, such as collision avoidance ones, could be easily analysed; and many other applications [1][2]. To date, model-based systems engineering, and digital twins' development are still in their infancy. They require a comprehensive study, high fidelity models, advanced digital technology, unified rules for data management and their precision level [1][2].

Concerning the present investigation, the work on the simulator and data analysis is still ongoing, on-orbit experiments are still being performed and the simulator is still being developed. In the paper the main results obtained to date and the critical aspects detected are discussed, in terms of data processing obstacles, simulations' fidelity of reproduction and influence of uncertainties. The future updates suggested for the project are also presented.

The paper is divided as follows: in Section 2 the application case of the simulator is described, the goals for the on-orbit experiments and the contributions of the involved companies to the project are presented; Section 3 defines the first version of the simulator, its main blocks and models are explained and the validation procedure with in-flight data described. Section 4 includes the data analysis procedure, the main problems detected, the investigation work on their causes and the suggested solutions. In Section 5 the outcomes of the preliminary analysis described are discussed and the main conclusions summed up in Section 6.

2. Application

The attitude and orbit simulation tool design presented in this paper is developed to support an on-orbit mission experiment for testing of a novel engine technology in Space, and analysis of the results.

A new propulsion technology is currently tested in a Low Earth Orbit (LEO) mission, at approximately 540 km from the Earth surface. The engine is carried as payload of a carrier spacecraft and tests are performed as part of a wider mission plan and operation of the satellite. The work focuses on modelling and simulation of the expected on-orbit results, in terms of motion evolution of the carrier spacecraft in the engine on-condition. The goal of this work is the analysis of the in-flight data and the reconstruction of the engine thrust model. The primary objective is to assess positive operation of the novel technology and its performance repeatability.

The company developing the engine is Genergo. (genergo.space – Genergo); and the company responsible for the launch of the carrier spacecraft is D-Orbit (Satellite Launch and Deployment | D-Orbit (dorbit.space)). Responsible of the analysis and prediction of the on-orbit experiment is Politecnico di Milano (www.compass.polimi.it).

Genergo has developed a new type of engine (See Fig. 1) that positively passed certified microgravity and other tests on Earth. By using different principles, this engine can be used for in-space propulsion of different types of spacecrafts, from small up to significant masses.

Fig. 1. Genergo's first generation engine currently undergoing tests in Space.

The engine company provides information about the propulsor, such as the engine expected performance, based on ground tests. The working principle of the propulsor has never been tested on-orbit, so its operation and performance are uncertain. The thrust profile is expected to be variable in time, but, since there is no accurate characterisation of the same yet, it has been assumed constant in the simulations.

Rather than testing the engine as an orbit control technique, it was decided to test its application in the manipulation of the attitude of the carrier spacecraft. The first generation of the propulsor is expected to produce low thrust in this first set of experiments, due to the current working principle, where some technical constraints were present, and satellite's safety reasons. The engine is located at a side of the spacecraft and when it is turned on it is expected that the thrust generates a torque with respect to the Centre Of Gravity (COG) of the spacecraft. The propulsion direction has been taken as in Fig. 2, knowing the engine position inside the satellite. The company responsible for the spacecraft provides information about the carrier and the nominal orbit, that influences the space environment definition. The satellite is modelled as the parallelepiped shown in Fig. 2, with mean dimensions provided by D-Orbit, and two sets of solar panels attached to two external surfaces of the structure. Mass properties, including inertias and COG position, are estimated by the company before each experiment. The estimated values are affected by uncertainties in Table 1. Thermal, optical, and magnetic coefficients of the structure are estimated in ranges. All the parameters previously defined are fixed to nominal values in the simulations, to ease computations.

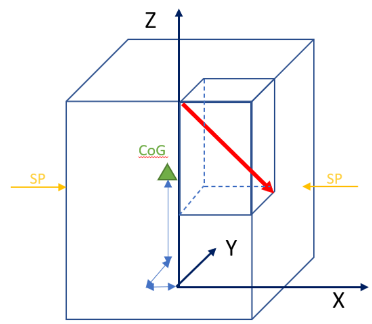

Fig. 2. Satellite parallelepiped model with visible internal payload case and thrust direction of the engine (red arrow). The figure also shows the satellite's reference frame (X, Y, Z axes) and the COG estimated position. Yellow arrows indicate the parallelepiped surfaces covered by Solar Panels (SP).

Table 1. Mass properties estimation uncertainties affecting the company measurements.

Parameter	Uncertainty
Satellite mass	±10%
Inertias	±10%
COG position	[Δx; Δy; Δz] = [±10; ±10; ±30] mm

The satellite company is responsible also of providing the telemetry data of the on-orbit tests. A standard format of the in-flight outcomes has been set. An example of it is given in Table 2.

Keeping in mind the primary goal of the mission, one test typically includes turn on of the engine, when the satellite moves in idle mode, and record of the telemetry. In principle, analysis of in-flight data with the simulator would allow to obtain a mean thrust magnitude during the experiment. The engine performance was not known a priori, so the detection capability of the instruments was not accurately tuned for the task.

Table 2. Example of the telemetry data format. Time is provided with precision up to seconds and data are sampled every 5 seconds, typically. For each data, its uncertainty is given.

Time	Position	Velocity	Angular velocity	Quaternions
Time (up to seconds)	$\boldsymbol{r}$±30 m	$\boldsymbol{v}$±0.01m/s	$\boldsymbol{\omega}$±0.005 °/s	$\boldsymbol{q}$±4 °
			$\boldsymbol{\omega}$±0.01 °/s (Eclipse)	$\boldsymbol{q}$±30 ° (Eclipse)

3. Attitude and orbit simulator

In its preliminary version, the simulator is designed to propagate in time both orbital motion and attitude dynamics of a satellite, by dealing with real telemetry data, which are used to input the initial conditions and tune the simulator parameters.

The on-orbit experiments are performed in idle mode of the satellite, so the satellite is not controlled actively, but moves freely under the environmental effects. Consequently, no control logic is included in the digital tool. Ideally, if the simulator represented the Space environment perturbations accurately enough, the effect of an additional engine thrust on the telemetry data would be observed. The simulator has modular structure and allows for future expansions and updates to enlarge its range of applicability.

The simulation tool is developed within the MATLAB® environment. A scheme representing the main simulator's blocks and their mutual connections is presented in Fig. 3. The code includes functions to model the perturbations and propagate the dynamics. Another script defines the satellite model, its main structure and mass parameters, and it should be adapted to each situation analysed. In the main interface, all the necessary functions to define the satellite, the environment and to propagate the motion are activated. The user can select the active environment perturbations, choose the simulation time and conditions, or set the input parameters.

The simulator propagation exploits MATLAB '*ode113*' variable-step, variable-order Adams-Bashforth-Moulton solver, and it appears to perform well in terms of accuracy and time. The telemetry data are used to set the initial conditions.

The modelled dynamics is now presented.

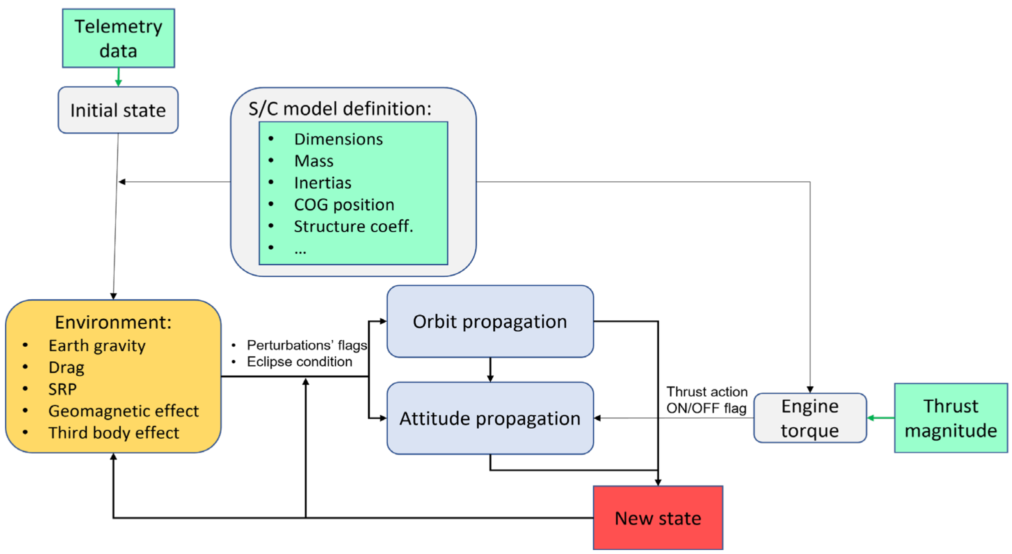

Fig. 3. Scheme of simulator's elements up to date. Green squares are the user defined inputs: telemetry data, satellite properties and estimated thrust magnitude. The grey boxes are the elements automatically computed by the simulator from external inputs: the satellite initial state and spacecraft rigid body model, and engine torque. The yellow box represents the environment, that includes both orbit and attitude perturbations calculations. The orbit and attitude dynamics propagators are given as blue boxes. Finally, the new state of the satellite, computed in a time step and saved as result, is given in the red square, that closes the loop as new input to the simulator.

3.1 Orbital dynamics

The orbital motion is propagated integrating Equation (1), that defines the acceleration of the satellite's COG.

$$\boldsymbol{a}_{CG} = \boldsymbol{g}_{Earth} + \sum \boldsymbol{a}_{perturbations} \tag{1}$$

The main contribution is given by the Earth gravity field $\boldsymbol{g}_{Earth}$, which is obtained from a potential model that considers the planet's oblateness. The gravity geopotential is modelled with expansion in spherical harmonics following the model described in [3] and exploiting the coefficients from GRACE gravity model 05 (GGM05s).

The orbital acceleration also considers the major environmental perturbations in LEO: atmospheric drag, solar radiation pressure and third body effect of the Sun and the Moon.

Atmospheric drag is modelled as in Equation (2) [4], where $\frac{A_{cross}}{mass}$ is the satellite cross section to mass ratio, C_d is the satellite drag coefficient, ρ is the estimated atmosphere density at the orbit altitude and $\boldsymbol{v}_{rel}$ is the relative velocity vector between satellite and atmosphere.

The atmosphere density is obtained from the MATLAB mathematical representation of the 2001 United States Naval Research Laboratory Mass Spectrometer and Incoherent Scatter Radar Exosphere (NRLMSISE-00) of the MSIS® class model, that has validity up to 1000 km from Earth surface and Space weather coefficients are taken from Celestrack [5] and are regularly updated.

$$\boldsymbol{a}_{drag} = -\frac{1}{2}\frac{A_{cross}C_d}{mass}\rho v_{rel}{}^2\hat{\boldsymbol{v}}_{rel} \qquad (2)$$

Solar radiation pressure effect is represented through the cannonball model of Equation (3) [4], which is an acceptable assumption given the orbital position and that there are no solar panels as flexible appendages. In Equation (3) p_{srp} is the solar pression computed as the ratio between radiation intensity and light speed, $\frac{A_{cross}}{mass}$ is the cross section to mass ratio, C_r is the satellite reflectivity coefficient and $\hat{\boldsymbol{r}}_{sc-sun}$ is the unit position vector of the Sun with respect to the satellite COG. Radiation intensity reaching the satellite includes the direct Sun radiation effect, estimated to be 1358 $\frac{W}{m^2}$, and the reflected and emitted Earth albedo at approximately 500 km from Earth for the case at hand.

$$\boldsymbol{a}_{srp} = -p_{srp}\frac{A_{cross}C_r}{mass}\hat{\boldsymbol{r}}_{sc-sun} \qquad (3)$$

Considering the large distance between the satellite orbiting the Earth with Sun and Moon, the typical central gravity model is applied to implement the attraction of third bodies. The orbital positions of Sun and Moon are computed at each time step with the analytical ephemerides' formulas in [6].

3.2 Attitude dynamics

The application in Section 2 aims at identifying the thrust action of an attitude engine. So, focus is set on the propagation of the attitude motion in principal axes of inertia. The angular velocity evolution is defined by the Euler's equations for a rigid body (Equation (4)) and the attitude evolution is obtained from the quaternions' kinematics (Equation (5)).

$$\boldsymbol{J}\dot{\boldsymbol{\omega}} + \boldsymbol{\omega} \times \boldsymbol{J}\boldsymbol{\omega} = \boldsymbol{T}_d + \boldsymbol{T}_u \qquad (4)$$

$$\dot{\boldsymbol{q}} = \frac{1}{2}\begin{bmatrix} 0 & \omega_z & -\omega_y & \omega_x \\ -\omega_z & 0 & \omega_x & \omega_y \\ \omega_y & -\omega_x & 0 & \omega_z \\ -\omega_x & -\omega_y & -\omega_z & 0 \end{bmatrix}\boldsymbol{q} \qquad (5)$$

Where $\boldsymbol{J}$ is the inertia tensor of the satellite, $\dot{\boldsymbol{\omega}}$ is the angular acceleration vector, $\boldsymbol{\omega}$ is the angular velocity vector, $\boldsymbol{T}_d$ is the total torque effect caused by the environment and $\boldsymbol{T}_u$ includes additional torques, such as the engine action. In Equation (5) $\dot{\boldsymbol{q}}$ is the quaternions' rate of change and $\boldsymbol{q}$ defines the quaternions' vector.

Gravity gradient torque $\boldsymbol{T}_{d_{GG}}$ is defined by Equation (6), following the model and approximations in [7], where μ_{Earth} is the Earth gravitational parameter, r is the position vector norm of the satellite with respect to the Earth, J_{ii} are the inertia parameters and c_1, c_2, c_3 are the direction cosines of the radial direction in principal axes. The atmospheric drag and solar radiation pressure torques, $\boldsymbol{T}_{d_{drag}}$ and $\boldsymbol{T}_{d_{srp}}$, consider the contribution of each -i^{th} external surface of the satellite structure from Equations (7) and (8) [7], where $\boldsymbol{r}_i$ is the position vector to each external surface and $\boldsymbol{F}_{i_{drag/srp}}$ is the perturbing force acting on each external surface. Equations (7) for the computation of $\boldsymbol{F}_{i_{drag}}$ include the drag coefficient C_d, the estimated atmosphere density ρ, the relative velocity of the satellite with the atmosphere $\boldsymbol{v}_{rel}$, Equation (8) for the computation of $\boldsymbol{F}_{i_{srp}}$ includes the solar pressure p_{srp}, the coefficients for diffuse and specular reflection for each external panel, C_{diff_i} and C_{spec_i}, and the Sun position vector from the spacecraft $\boldsymbol{r}_{sc-sun}$. A_i is the cross-sectional area and $\boldsymbol{n}_i$ is the normal vector of each external surface. Finally, also the geomagnetic field ($\boldsymbol{b}$) interaction with the residual magnetic dipole ($\boldsymbol{m}$) of the satellite is computed ($\boldsymbol{T}_{d_{mag}}$) and added to the environmental torques from Equation (9) [7]. The effects act on the COG of the satellite, assuming the structure of Fig. 2 and that the centre of pressure of each surface equals the geometric centre. The geomagnetic field definition exploits the International Geomagnetic Reference Field (IGRF2020) model.

$$\boldsymbol{T}_{d_{GG}} = \frac{3\mu_{Earth}}{r^3}\begin{cases}(J_{zz} - J_{yy})c_2c_3 \\ (J_{xx} - J_{zz})c_1c_3 \\ (J_{yy} - J_{xx})c_2c_1\end{cases} \qquad (6)$$

$$\boldsymbol{T}_{d_{drag}} = \sum \boldsymbol{r}_i \times \boldsymbol{F}_{i_{drag}}$$
$$\boldsymbol{F}_{i_{drag}} = -\frac{1}{2}C_d\rho v_{rel}{}^2A_i\max(\hat{\boldsymbol{n}}_i \cdot \hat{\boldsymbol{v}}_{rel}, 0)\hat{\boldsymbol{v}}_{rel} \qquad (7)$$

$$\boldsymbol{T}_{d_{srp}} = \sum \boldsymbol{r}_i \times \boldsymbol{F}_{i_{srp}}$$
$$\boldsymbol{F}_{i_{srp}} = -p_{srp}A_i[2\left(\frac{C_{diff_i}}{3} + C_{spec_i}(\hat{\boldsymbol{n}}_i \cdot \hat{\boldsymbol{r}}_{sc-sun})\hat{\boldsymbol{n}}_i\right. \\ \left. + \left(1 - C_{spec_i}\right)\hat{\boldsymbol{r}}_{sc-sun}\right]\max(\hat{\boldsymbol{n}}_i \\ \cdot \hat{\boldsymbol{r}}_{sc-sun}, 0) \qquad (8)$$

$$\boldsymbol{T}_{d_{mag}} = \boldsymbol{m} \times \boldsymbol{b} \qquad (9)$$

A better resolution of the shape and of the mass distribution of the satellite would refine the results of the applied torques' effects. Solar radiation pressure has been considered only when the satellite is not in eclipse condition, which is analytically computed from Line-Of-Sight geometry computation at each step [6].

Environmental effects depend on coefficients that model the characteristics of the satellite's structure, such as the reflectivity coefficient C_r, the drag coefficient C_d, the specular and diffuse reflection coefficients C_{spec} and C_{diff}, the area to mass ratios $\frac{A_{drag/srp}}{mass}$ for drag and solar radiation pressure effects and the residual magnetic dipole $\boldsymbol{m}$. These parameters are difficult to estimate, but when dealing with a real spacecraft, they can be approximated from mechanical and optical properties of the structure. Area to mass ratios have been obtained from estimated satellite and mass dimensions, within uncertainties; the coefficients are variable and can be computed only in ranges.

It was expected and confirmed by the results that inertias play a significant role in the attitude simulation outcome. Differently, perturbing actions have minimal effect on the dynamics, due to the short duration of the experiments to analyse, that do not account for long-term variations of the motion caused by the environment. So, the motion evolution is not sensible to the variation of satellite's coefficients for environment interaction definition. Some nominal values have been selected.

3.3 Validation

Validation of the simulator has been performed before the launch of the mission of Section 2, so the telemetry data exploited refer to a previous mission of a similar satellite, in terms of operative orbit and satellite's dimensions, with no external engine thrust included. Structural coefficients' ranges, dimensions and mass properties have been provided by the satellite company. This reference telemetry used for validation is hereafter referred as EXP1.

The simulated motion has been validated first by checking the models and their applicability with the literature. Each perturbing action has been validated by comparison with literature results, in terms of order of magnitude of the effects in similar regions of the Space from [8].

The overall propagator behaviour has been checked comparing the results of the simulations and the telemetry data of the satellite moving in space under the effect of Space environment only.

The orbit dynamics was found to be adequately reproduced, as shown in Fig. 3 where the continuous line represents the model while the dotted line the data for orbital position and velocity.

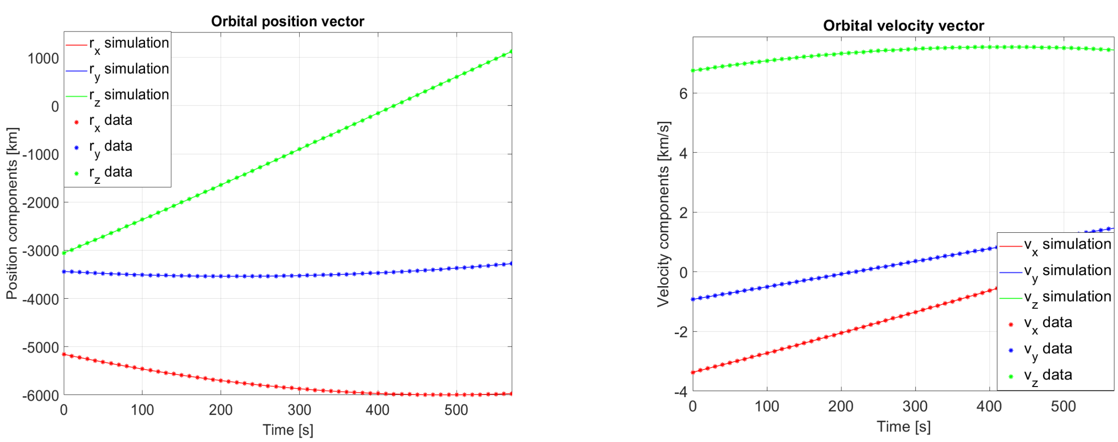

(a) Zoom of EXP1 orbital position components data (*) and simulation outcome (-).

(b) Zoom of EXP1 orbital velocity components data (*) and simulation outcome (-).

Fig. 4. Orbital position and velocity components telemetry data of EXP1 (*) and simulator reproduction (-) comparison in the same graphic. The orbital motion is propagated in Earth Centred Inertial (ECI) frame, the initial state is provided by telemetry data at that epoch, the time along the x-axis is the simulation time.

Differently, as expected, the attitude dynamics has been found more difficult to reproduce. During one simulation it is observed accumulation of error due to the many approximations and uncertainties introduced in the simulator, as shown in Fig. 5(a). This is due to the uncomplete knowledge of the carrier spacecraft and the fact that it is modelled as a simple parallelepipedal shape with constant density.

Consequently, two important optimisation phases are required in the analysis, a preliminary one on some fundamental physical parameters to adapt the simulator to the current mission conditions and reach acceptable level of data simulation in torque-free motion. The second optimisation performed is the real reverse engineering approach to compute the thrust of the engine necessary to fit the angular velocity telemetry with the simulations.

Phase one of this optimisation procedure has been performed on inertias and initial conditions within their estimation errors. These parameters were expected to be the most relevant ones on the attitude evolution, as confirmed by the analysis described in Section 4.3.
Both optimisation phases, on inertias and initial angular velocity first and on thrust later on in the analysis, exploited the non-linear curve fitting of data in a least squares sense applying the default thrust-region-reflective algorithm of MATLAB '*lsqcurvefit*' function to match the attitude data. The optimisation works on a non-linear constrained problem, the parameters are varied within their estimation and measurement errors.

The best sequence of parameters optimisation was not known a priori, so many combinations have been run. Even if the uncertainty ranges of the varied parameters did not allow a successful fitting on the dynamics, the best approximation of the data was sought for. Fig. 5(b) shows the results obtained optimising the inertias and the initial angular velocity, that had the major influence on the results. The angular velocity data fitting has been privileged over the quaternions fitting. In fact, the angular velocity dynamics is more reactive to the engine effect.

The validation proved how the simulator can model the general orbit and attitude dynamics of the satellite, but it is necessary to preliminarily tune some parameters within their estimation ranges. Each calibration and optimisation have been selected and manually performed; in future updates it would be useful to automate the procedure.

3.3.1 Engine experiment mission

Fig. 6(a)-(c) show the outcomes of the same tuning procedure but applied to the mission described in Section 2. Telemetry data refer to satellite torque-free motion and are hereafter referred to as EXP2. Orbital motion is reproduced accurately enough with default data for the environmental coefficients and initial conditions equal to the recorded telemetry. Differently, as the validation procedure highlighted, attitude motion required optimisation of the most influent parameters: inertias and initial condition of angular velocity. The results in Fig. 6(c), (d) are obtained before and after optimisation.

3.3.2 Critical aspects of the on-orbit experiment

Critical aspects of dealing with real telemetry data came out during validation procedure of the simulator.

Consistency of reference frames is necessary to adequately compare the simulator outcomes and the satellite data.

Telemetry data are noisy (see Fig. 7). This has a critical effect on the definition of the initial state of the satellite. The figure gives an idea of the estimation error of the angular velocity, in accordance with the data in Table 2. Moreover, outliers need to be filtered and a gap in the telemetry is clearly visible.

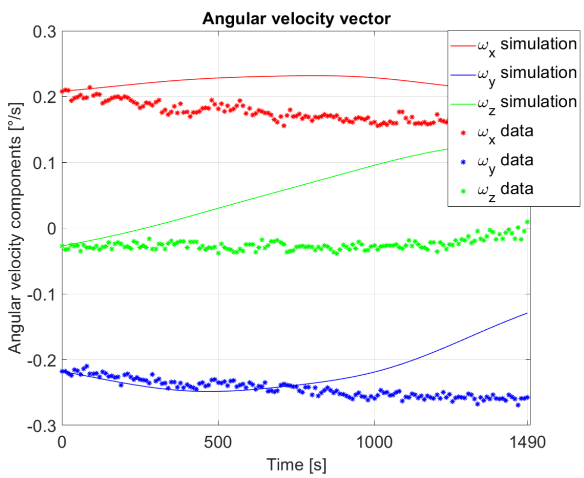

(a) EXP1 angular velocity components data (*) and simulation outcome (-), no optimisation performed.

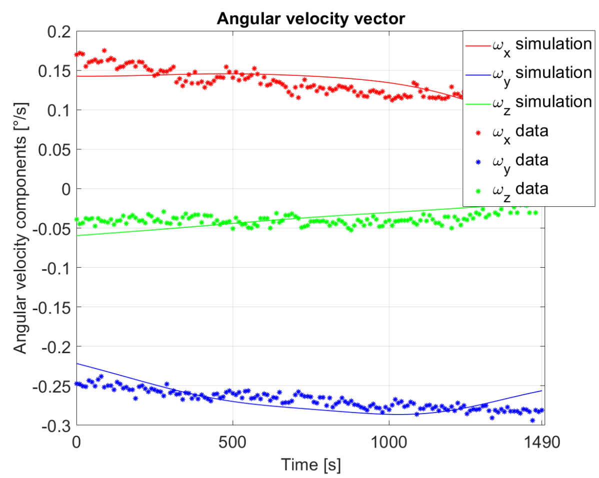

(b) Angular velocity telemetry data of EXP1 (*) and simulator reproduction (-). Optimised inertias and initial angular velocity.

Fig. 5. Angular velocity data of EXP1 (*) and simulator reproduction (-) comparison in the same graphic. Both are given in principal body coordinates of the satellite, the initial state is provided by telemetry data at that epoch, the time along the x-axis is the simulation time.

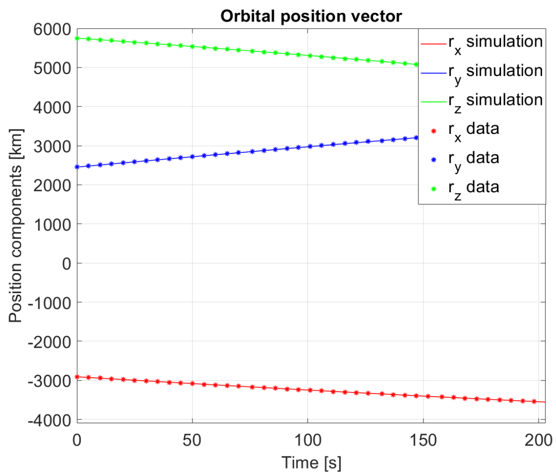

(a) Zoom of EXP2 orbital position components data (*) and simulation outcome (-).

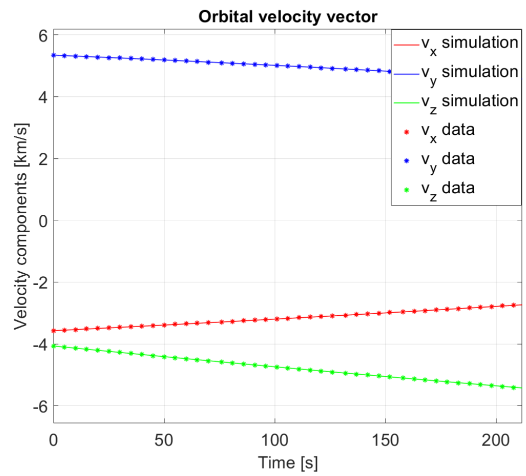

(b) Zoom of EXP2 orbital velocity components data (*) and simulation outcome (-).

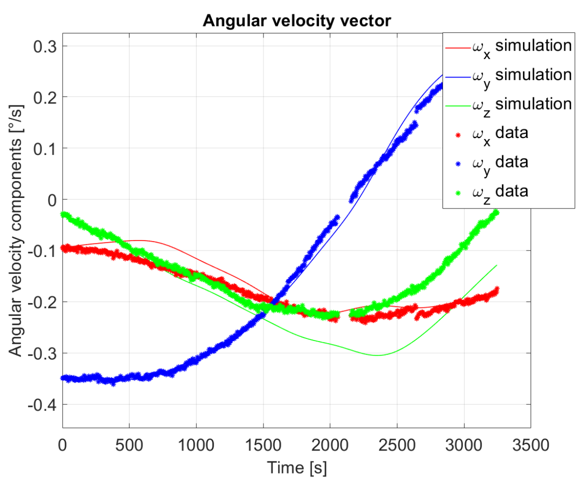

(c) EXP2 angular velocity components data (*) and simulation outcome (-). No optimisation has been performed on the default physical parameters provided by the satellite company.

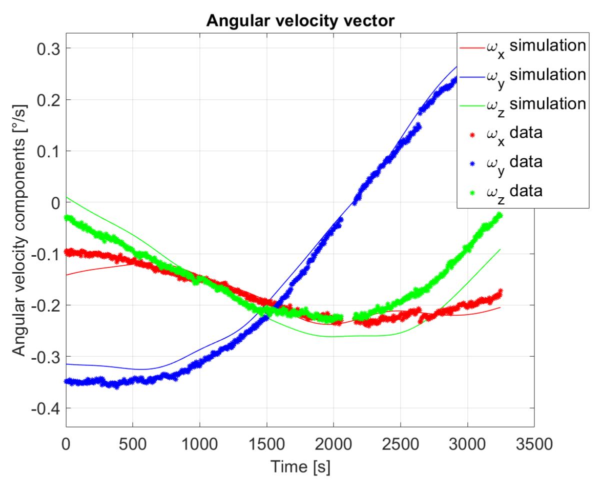

(d) EXP2 angular velocity components data (*) and simulation outcome (-). Inertias' values and initial angular velocity optimised within their uncertainty ranges.

Fig. 6. Orbital position (a), velocity (b) and angular velocity (c) components' telemetry data of EXP2 (*) and simulator reproduction (-), comparison in the same graphic. The orbital motion is propagated in ECI frame, angular velocity components are given in principal body coordinates of the satellite, the time along the x-axis is the simulation time. Zoom of orbital position and velocity are shown in figures (a) and (b). Comparison between figures (c) and (d) shows the beneficial effect of the preliminary optimisation of the simulator's most influent physical parameters. (Quaternion data are not considered because the telemetry was badly affected by discontinuities)

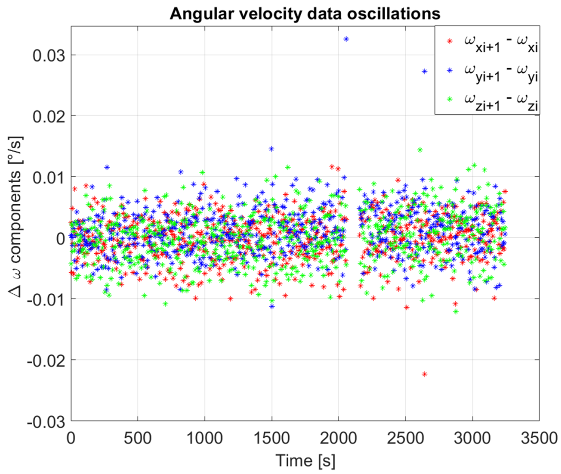

Fig. 7. EXP2 data oscillations of the angular velocity components between successive sampled time instants. From telemetry data, each point (*) shows the difference $\omega_{i+1} - \omega_i$ for each component. EXP2 does not include the thrust action of the engine.

For the case at hand, quaternions data showed some discontinuities while the simulator results did not. It is probably caused by a different interpretation of the attitude at a given time by the satellite logic and the simulator. This should be further investigated in collaboration with the satellite company. In future updates this gap of information about interpretation of quaternions should be filled to exploit attitude knowledge during the experiment and improve attitude reproduction with the simulator.

The noise of the data output has not been reproduced and the control action of the satellite has not been modelled, since the analysed experiments have been performed in idle mode.

Future updates will expand the capabilities of the simulator by creating modules of standard controllers, actuators, and reference to track. Each module will be enabled through the main code interface and added to the loop. Consequently, the simulator will become a useful tool for a broader range of missions and experiments, both before, during and after the on-orbit phase, to investigate, plan and analyse the operations.

4. Data analysis procedure

The work described in the paper aims at analysing telemetry data of on-orbit experiments to assess the operativity of a novel engine technology. The analyses are currently in progress and are carried on in close cooperation with the satellite and the engine companies.

During a typical experiment the control logic of the satellite is turned off, then the payload engine starts and generates thrust for a defined duration. At the end of the firing phase the engine stops and after some time the satellite goes back to its default-controlled motion.

The duration of each phase and the engine working configuration vary between different sets of tests. The operations are defined on-going of the mission.

4.1 Ideal procedure

The expected workflow to analyse the data and the expected outcome of the work would be the following (see Fig. 8):

1. On-orbit experiment and download of telemetry data of all the phases.
2. Automatic process of the telemetry data and graphic rendering. Preliminary investigation of changes in the attitude caused by the engine. In particular, the angular velocity data should show discontinuities when the payload is turned on and off. An example of what should be obtained is given in Fig. 9: a nominal thrust effect has been added to the simulation of EXP2 conditions. The simulator's results show discontinuities when the engine is turned on and off.
3. Simulation of torque-free motion of the satellite. The orbit, satellite and engine parameters have been previously provided by the companies. The initial state of the carrier is set from the telemetry. Orbital and attitude motions are propagated with the simulator for the test duration, under the environmental influence only. In this step the engine thrust magnitude is unknown, its action is not included. The simulation should differ from the telemetry data. The results are compared with the telemetry and clear differences and motion deviations, when the engine is turned on and off, are sought for. However, as already found during validation, it is typically necessary to perform tuning of some uncertain parameters (see Fig. 8), that have significant effect on the performance of the simulator.
4. An optimisation procedure is exploited. In agreement with the satellite and engine companies, telemetry of the satellite in idle mode with no engine thrust, for some defined amount of time, is downloaded for this tuning purpose. The optimisation focuses on inertias' values within their estimation uncertainties in Table 1, and on the initial angular velocity within measurement noise provided in Table 2 and observed in Fig. 7. The most reactive measure to the thrust effect is the angular velocity, so the optimisation procedure aims at its data fitting. The numerical technique is the one in Section 3.3: data fitting in least-square sense. The procedure and results of this point have already been presented for the mission at hand in Section 3.3.1. After this first phase of optimisation on inertias and angular velocity initial state, the varied values are given as inputs to the simulator and the analysis of point 3 of the list is repeated.

5. Ideally, the simulator reproduces the main effects acting on the satellite's motion except for the engine thrust, at this stage. In principle, the thrust magnitude can be obtained from optimisation. The engine action is activated in the simulator within the firing time. The second phase of the optimisation procedure is carried out and data fitting of the angular velocity is performed varying the thrust magnitude, which is the only unknown to compute the torque in Equation (4).
6. The optimisation of point 5 should return the magnitude of the engine thrust applied during the experiment, according to the telemetry. As final check, this value is given as input to the simulator and the engine firing flag activated in the simulation. It is expected that the simulated motion follows closely the telemetry data of the experiment.

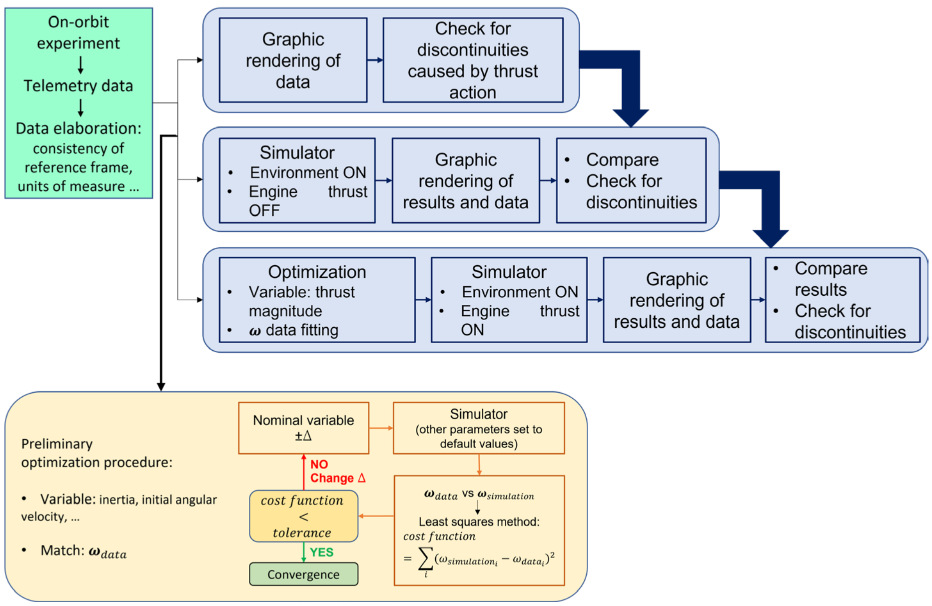

Fig. 8. Scheme of the ideal procedure of the analysis. From the on-orbit experiments the telemetry is obtained, and processed, to look for visible changes in the attitude caused by the engine. Then, the simulator is exploited to simulate the test and interpret the telemetry. From comparison of results, it should be visible the effect of the engine, if the payload successfully worked and its effect was detectable. However, the simulator requires a preliminary tuning to adapt to the current conditions of the satellite and to deal with measure uncertainties.

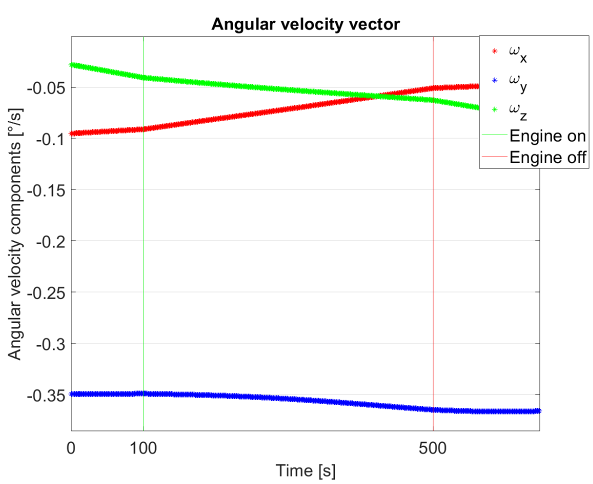

Fig. 9. Example of how the angular velocity evolution should look like in a test. Data are simulated from orbit and satellite conditions of EXP2, adding engine firing between 100 and 500 s of the simulation time (x-axis). The simulator considers a constant thrust profile, directed as in Fig. 2, and thrust magnitude assumed 10^{-4}N.

4.2 Detected problems

Often the optimisation, on simulator parameters and thrust magnitude, did not converge and a significant gap between data and simulations could not be filled following the procedure of Section 4.1. This is probably due to the low value of the thrust magnitude, expected for the specific engine configuration of the mission in Section 2, which is the first generation of the propulsor, due to some technical constraints and safety reasons.

Consequently, a different approach has been applied to investigate the causes of this. Many optimisation attempts have been performed on many different experiments, to set the initial parameters of the simulator for each test and then obtain the thrust action. Since convergence of results was hard to obtain, aim was to infer statistical estimates of the variables.

As a reference, for this first configuration of the propulsor system the engine thrust order of magnitude is assumed to be in the range 10^{-4}-10^{-6} N, that causes a torque effect in the order of 10^{-5}-10^{-7}Nm, according to the thrust direction and constant profile defined in

Section 2. It must be pointed out that the satellite properties and state vary in each test and affect the results on the engine performance. The orders of magnitude and the results provided in this Section refer to a batch of engine experiments, hereafter referred to as EXP3, to distinguish it from the torque-free data of EXP2 of the same mission.

Possible causes to the difficult convergence of the optimisation and to the difficult observability of the thrust have been considered.

The thrust effect for this first-generation engine may be too small and covered by the residual dynamics not reproduced in the simulator; the excessive noise of the angular velocity data may cover the motion deviations caused by the engine and the filters may cause some unexpected effect on the data; the assumption of constant thrust may be too simplistic.

4.3 Problems investigation with different approach

Aim of the work presented in this Section is to infer and roughly quantify the main approximations and uncertainty effects on the simulator.

The approach exploited Equation (4) for attitude dynamics of a rigid body. Starting from a set of telemetry data, Equation (4) has been solved to obtain the $\boldsymbol{T}_u$ contribution, given as input the current state of the satellite and the environmental disturbance torques at that time and position in Space, computed with the simulator. Ideally, the simulator represents all the relevant effects of the environment, so the resultant torque would be mainly the engine thrust action, when present, or zero in torque-free motion. In reality, $\boldsymbol{T}_u$ includes all the residual effects that the simulator does not consider.

To assess the limitations of the simulator, a set of fictitious telemetry data has been generated. Given an initial state and default parameters of the satellite from EXP3, the dynamics have been propagated for one orbital period and the telemetry obtained each second, including angular accelerations. The data were punctually exact, no sensor noise is reproduced in the simulator. Moreover, no environmental torques have been included, to ease and speed up computations.

The method has been validated giving the fictitious torque-free data as input in Equation (4) to obtain the residual torque $\boldsymbol{T}_u$. The result was close to zero, limited by computation accuracy.

The set of data has been used to roughly quantify the effect of uncertainties. Artificial noise has been added to the angular velocity: random variation of each point within the uncertainty range. The results are in Fig. 10.

Then, the noisy data have been given as input to Equation (4), that has been inverted to obtain the residual effect introduced by the non-filtered noise. Results in Fig. 11 show how the residual torque norm has order of magnitude comparable to the expected torque caused by the engine, assumed in the analysis.

Filters and smoothing methods can process noisy data (see Fig. 12). Choosing the correct filtering method and adapt it to the case at hand has a non-negligible influence on the simulation outcome. Fig. 13 shows the resulting residual torque norm obtained inverting Equation (4), given the noisy angular velocity previously generated and processed with a low-pass filter.

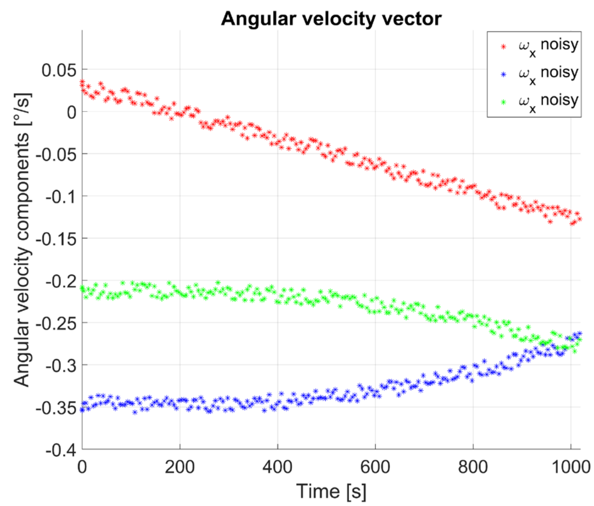

Fig. 10. Noisy angular velocity fictitious set of data, zoom. From orbit and satellite's conditions of EXP3, the simulator propagated the angular velocity over one orbital period. Then, noise has been added to each point, sampled every 1 s, as random variation within ±0.01 °/s.

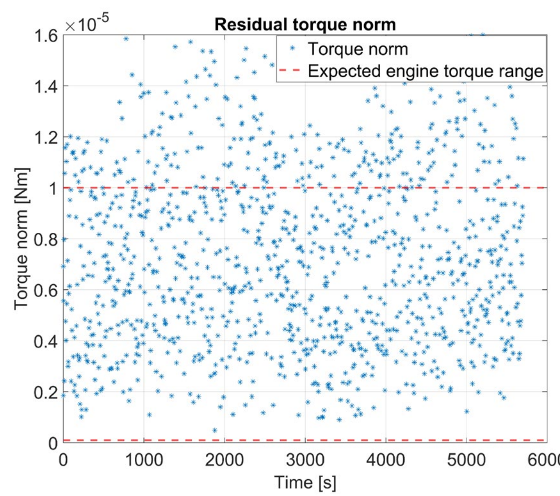

Fig. 11. Residual torque norm obtained inverting Equation (4) from noisy data (see Fig. 10), compared with the expected torque range of the tested engine (interval within red dotted lines). The figure shows the effect of noise on the residual torque obtained.

The residual torque obtained is still very large, too much to detect the thrust action expected. The main settings of the filter should be accurately tuned. Moreover, filtering may introduce some pattern in the resulting torque, caused only by numerical effects. It must not be considered a physical phenomenon when dealing with real filtered data. Fig. 14 shows an example of numerical pattern in the results caused by the better smoothing of data with MATLAB '*rloess*' method previously defined.

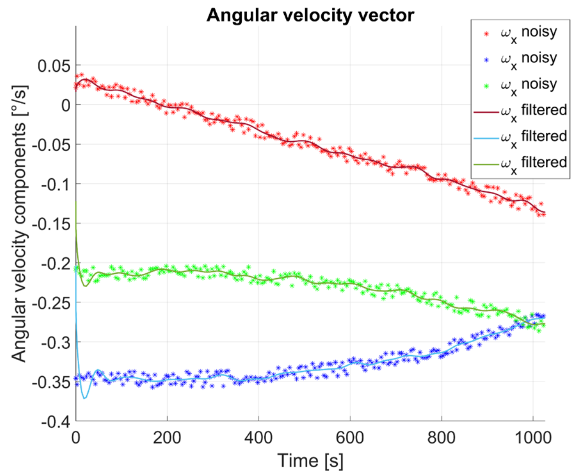

Fig. 12. Low pass filter smoothing effect on the noisy angular velocity, generated with the simulator (see Fig. 10).

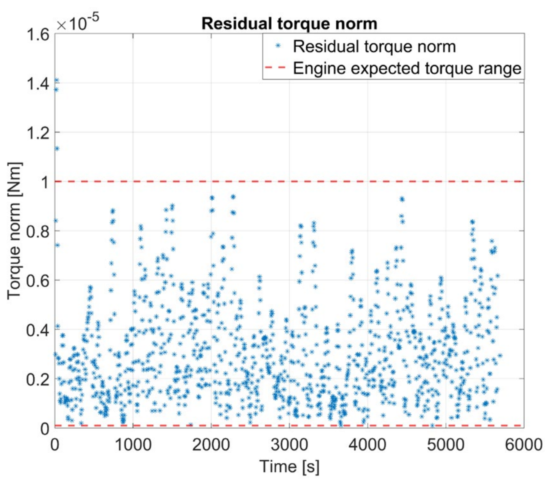

Fig. 13. Residual torque norm obtained inverting Equation (4) from noisy data filtered (see Fig. 12), compared with the expected torque range of the tested engine (interval within red dotted lines). The figure shows the effect of noise and filter on the residual torque obtained.

When the inversion of the dynamics method at each sample time is applied directly to the noisy telemetry downloaded from the satellite during the test (EXP3), an additional modelling error must be introduced: the approximation of the angular acceleration at each time step. In fact, telemetry does not report the angular acceleration of the satellite, which is a necessary input to invert Equation (4) and obtain the residual $\boldsymbol{T}_u$ that includes: the residual dynamics non-modelled in the simulator, the effects due to approximations and estimation errors and the engine torque tested. Once again, to quantify the angular acceleration approximation error, the fictitious set of data previously generated with filtered noise, is given as input to Equation (4), but the angular velocity derivative is approximated with finite differences methods: forward and central differences between consecutive samples, see Equations (10) and (11), respectively, where $\dot{\boldsymbol{\omega}}_i$ is the angular acceleration at the current time step t_i and $\boldsymbol{\omega}_{i-1}$, $\boldsymbol{\omega}_i$, $\boldsymbol{\omega}_{i+1}$ are the angular velocities at the previous (t_{i-1}), current (t_i) and next (t_{i+1}) time steps.

$$\dot{\boldsymbol{\omega}}_i = \frac{\boldsymbol{\omega}_{i+1} - \boldsymbol{\omega}_i}{t_{i+1} - t_i} \qquad (10)$$

$$\dot{\boldsymbol{\omega}}_i = \frac{\boldsymbol{\omega}_{i+1} - \boldsymbol{\omega}_{i-1}}{t_{i+1} - t_{i-1}} \qquad (11)$$

The residual torque has been computed at each time instant of the data and the results are in Fig. 15.

The same approach has been applied to the real telemetry data of EXP3. The angular velocity data, smoothed with the robust quadratic regression over each sliding window of samples method, MATLAB function 'rloess' of Fig. 16(a), have been given as input to Equation (4), the angular acceleration has been approximated with central finite differences from Equation (11), and the residual torque $\boldsymbol{T}_u$ has been obtained and shown in Fig. 16(b).

Consequently, this method cannot be applied to directly obtain the engine torque from $\boldsymbol{T}_u$, too many approximations and numerical errors affect the data and the simulator. However, the approach has been exploited to perform a sensitivity analysis to some physical variable parameters, which are expected to influence the most the attitude evolution: inertias, COG position, mass and residual magnetic dipole of the satellite. Aim was to infer if changes in some physical parameters affect the residual torque.

The values of the parameters defined before have been randomly varied within their uncertainty intervals and many simulations run to obtain statistical results, 5-10 simulations per parameter proved to be enough to show presence or not of relevant effects.

As expected, inertias resulted to be the only property with a clear influence on the residual torque, as shown in Fig. 17. Differently, COG position, mass and residual magnetic dipole did not have any relevant effect. In conclusion, inertias are the parameters that influence the most the attitude dynamics, accurate estimates of their values can improve the simulation, significantly reducing the residual dynamics error.

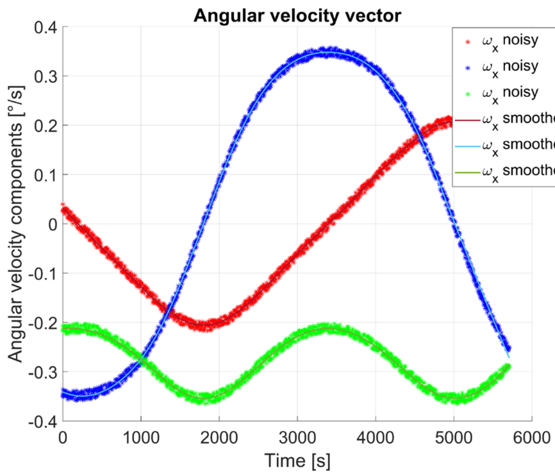

(a) Example of noisy angular velocity data (*), generated with the simulator from orbit and satellite conditions of EXP3 adding noise (see Fig. 10), smoothed applying function '*smoothdata*' and method '*rloess*'. The filtered data are the continuous lines (-).

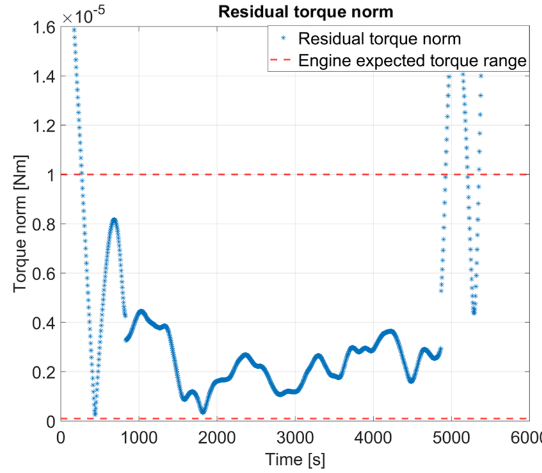

(b) Residual torque norm obtained inverting Equation (4) from the noisy data smoothed in (a), compared with the expected torque range of the tested engine (interval within red dotted lines). It can be noticed how the smoothing effect causes a pattern in the torque norm obtained, it is caused by numerical effects and must not be interpreted as a physical phenomenon.

Fig. 14. Example of the effect of smoothing of data on the resulting residual torque norm, obtained inverting Equation (4) at each time step. A pattern appears in the results, which is only caused by the numerical action of the filter.

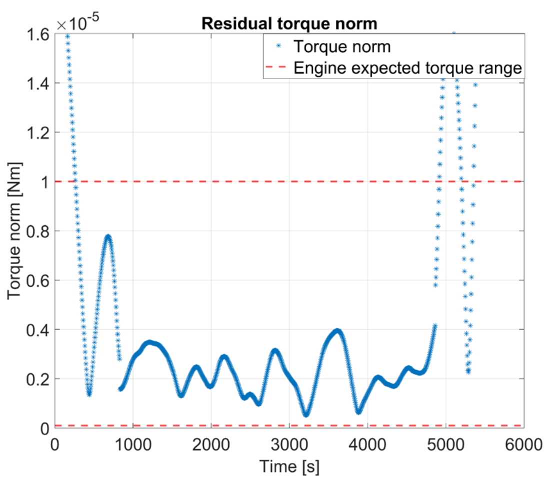

(a) Residual torque norm obtained inverting Equation (4), from the noisy data generated from orbit and satellite conditions of EXP3, smoothed as in Fig. 14, compared with the expected torque range of the tested engine (interval within red dotted lines). The angular acceleration has been approximated applying forward finite differences at each time step.

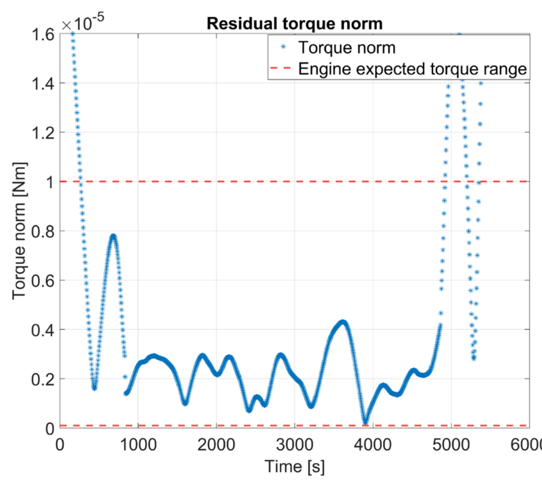

(b) Residual torque norm obtained inverting Equation (4), from the noisy data generated from orbit and satellite conditions of EXP3, smoothed as in Fig. 14, compared with the expected torque range of the tested engine (interval within red dotted lines). The angular acceleration has been approximated applying central finite differences at each time step.

Fig. 15. Residual torque norm obtained inverting Equation (4) and approximating the angular acceleration, at each time step, with forward (a) and central (b) finite differences. The input data are the fictitious angular velocity generated with the simulator from conditions of EXP3, to which noise has been artificially added and smoothed (see example Fig. 14).

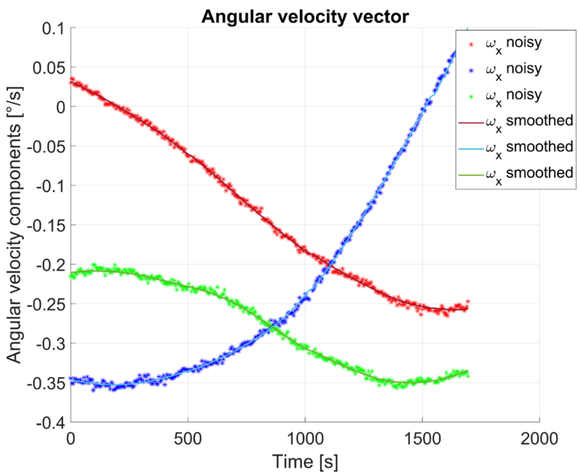

(a) Example of noisy angular velocity data (*), from the real telemetry data of EXP3, smoothed applying function '*smoothdata*' and method '*rloess*'. The filtered data are the continuous lines (-).

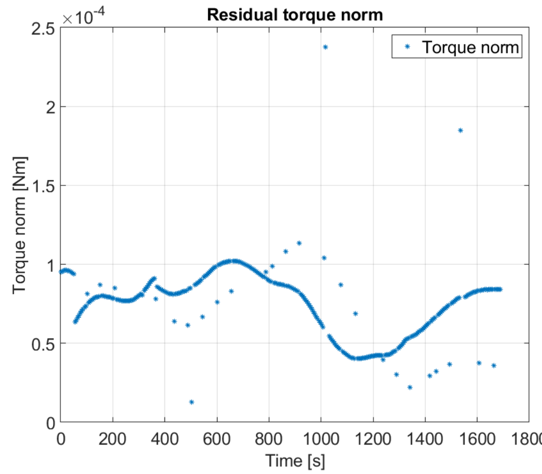

(b) Residual torque norm obtained inverting Equation (4) from the noisy data smoothed in (a).

Fig. 16. Example of angular velocity telemetry from EXP3 smoothing and residual torque obtained applying the direct inversion of Equation (4).

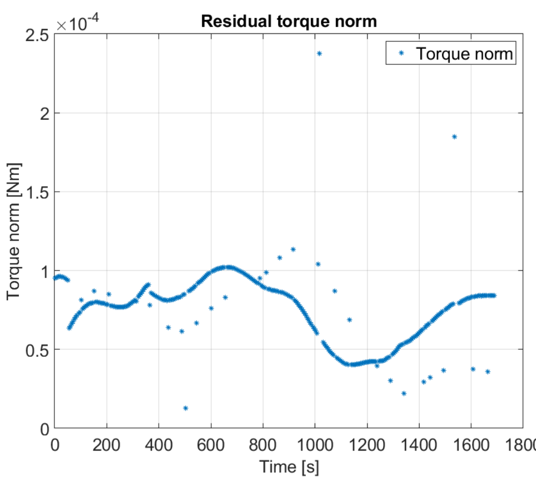

(a) Residual torque norm obtained inverting Equation (4), from the real telemetry data of EXP3, smoothed as in Fig. 16(a). Same results as in Fig. 16(b). Nominal inertias values.

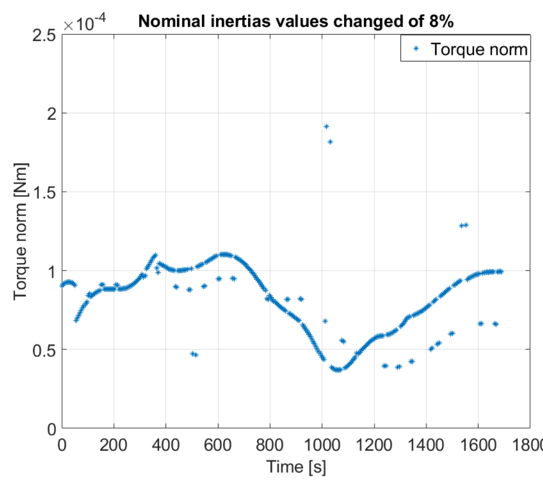

(b) Residual torque norm obtained inverting Equation (4), from the real telemetry data of EXP3, smoothed as in Fig. 16(a). Inertias changed of 8% from nominal values.

Fig. 17. Effect of satellite's inertias on the residual torque norm, obtained inverting Equation (4). Comparison between the residual torque norm obtained with nominal inertias values and changed ones within uncertainties.

4.4 Results

The simulator designed up to date includes the orbital and attitude motions' propagation through the Space environment's main effects. The perturbing forces are modelled with typical methods and the payload engine thrust action can be included, but it is approximated as constant in magnitude and direction.

Simulation of satellite evolution, with initial state set from noisy telemetry, does not match the attitude data. The system's parameter identification through an optimisation approach requires further improvement to account for the observed issues.

Considering Genergo first generation engine mounted on the carrier spacecraft, the existing technical constraints and the resulting working configuration in low-thrust mode, the expected order of magnitude of the engine torque, in the analysed set of tests EXP3, is around 10^{-5}-10^{-7}Nm. The residual torque magnitude, that the simulator does not consider, ranges around 10^{-4} - 10^{-6}Nm. The main cause of it is the noise of the data measurements, it is so large that the engine effect is not detectable. This problem will be solved in following on-orbit experiments, by changing the engine configuration and reducing the measurement errors.

Filtering the noise with typical approaches has been proved beneficial and an accurate tuning of the smoothing method is necessary. However, some pattern in the filtered data may appear for numerical effects of the smoothing action. Advanced filters should be applied and adequately tuned.

The sensitivity of the simulation to some physical parameters has been investigated and the most influent properties on the attitude resulted to be the values of the inertias. So, it is necessary to accurately estimate them to improve performance of the simulator and reduce approximation errors.

4.5 Next steps

The simulator models the reality, residual effects caused by unmodelled dynamics and approximations are always present, however for the case at hand this contribution is comparable to the investigated torque.

The main problems affecting the analysis have been characterised and in future updates actions can be taken to improve simulator's performance and data analysis.

In accordance with the satellite company, the quality of the telemetry might be improved, and the noise level reduced. Attitude determination would be improved by also exploiting the information about quaternions during the experiment. The simulator should be made capable to automatically deal with quaternions' data discontinuities, fixing the gap between interpretation of the telemetry and reproduction in the simulation.

Filtering may be improved with a dedicated analysis on the selection of the best filter option and on the settings of the filter parameters.

A model of the engine may be developed and included in the simulator loop. Moreover, in accordance with the engine company, different types of engines will be tested in other configurations capable of generating larger thrust magnitudes.

5. Discussion

The results presented in the paper are the outcomes of a first phase of analysis involving an orbit and attitude simulator, developed specifically to face the task of Section 2. The design of the tool is still in progress and the first version includes modelling of environmental perturbations and propagation of orbit and attitude motions. Peculiar is the telemetry in the loop of the analysis. Data sets of on-orbit experiments are processed and analysed to define the initial inputs to the simulator. The work done so far highlighted some important requirements and limitations to the on-going analysis and software development.

Telemetry is affected by noise that should be adequately filtered. The filter applied to the data should be specifically selected and set for the task at hand, so a preliminary characterization of the same is necessary. From the many experiments analysed applying the ideal procedure of Section 4.1, it has been observed the significant influence of fine definition of the initial state of the satellite, in particular of the initial angular velocity. In fact, the angular velocity is the most reactive parameter to the phenomenon investigated and the analysis focused on it. Noise of the data makes it difficult to clearly state the initial attitude, so it should be estimated through filtering action and optimised data fitting. Moreover, the results in Section 4.4 show how the noise level should be compatible with the range of the phenomenon investigated. To date, the angular velocity noise affecting the telemetry resulted far too large to easily detect the expected engine thrust effect.

Many assumptions and uncertainties have been introduced in the simulator. The sensitivity analysis in Section 4.3 helped identifying the inertias as the most influent parameters on the attitude outcome of the simulator, while other coefficients investigated had a negligible effect. Consequently, before the actual analysis, these parameters should be set and tuned, exploiting an optimisation procedure, to match the torque-free motion evolution of the satellite with the telemetry under the same conditions. This procedure must be repeated before each experiment since the parameters vary in time.

The optimisation approach exploited typically did not reached convergence. This shed light on the importance of implementing an accurate model of the phenomenon investigated. Future updates should include a more realistic representation of the engine.

The results discussed in the paper highlighted some problems and suggested future updates to both execution of experiments and design of the simulator.

Higher accuracy for telemetry and satellite's properties may be required in future experiments. Repeated tests are necessary to validate the simulator performance and to clearly assess the engine operation.

The digital tool developed is useful to investigate a phenomenon through data from on-orbit experiments. However, the work presented in the paper proved how the simulator is used also to characterise unexpected results of the analysis, detect possible causes to obstacles encountered and quantify the effect of different contributions to the dynamics.

6. Conclusion

Genergo has developed a novel engine technology that can be used for in-Space propulsion of different types of spacecrafts, by means of different principles. The company is interested in assessing engine operation and characterise performance of the same, in its various configurations, through on-orbit experiments. Currently, the engine is part of a satellite payload and tests are being executed to verify some basic construction designs. The engine is set to operate for a defined amount of time, satellite's telemetry is recorded and downloaded to ground, and it is processed and analysed by the authors. An orbit and attitude's simulator is under development and its preliminary version is presented in the paper. The simulator is coded in MATLAB and propagates orbit and attitude's dynamics of the satellite moving in idle mode in the Space environment. The tool takes as input orbit and satellite's conditions during a specific experiment and the initial state is set by the telemetry recorded. To date, the simulator can reproduce orbital motion and the general attitude behaviour of the satellite. However, a preliminary optimisation of influent physical parameters, mainly inertias and initial angular velocity, is necessary to match torque-free angular velocity data.

The procedure followed to detect the engine thrust highlighted some issues that have been characterised, and future improvements have been suggested. Critical aspects so far involve: telemetry data affected by sensors' noise, outliers and gaps in the acquisition; the limitations imposed by the sampling and downlink capabilities. Data noise is the main obstacle to the detection of the engine thrust, smoothing is necessary and requires tuning of the filter parameters, according to the case at hand. Many modelling errors and approximations are included in the simulator, such as the engine thrust modelled as constant.

Future updates applied to the simulator will improve its performance. The main problems affecting the analysis, that are presented in the paper, will be dealt with and the experiments campaign carried on. Engine developments will be configured and tested on future missions that are currently in the works.

The preliminary version of the simulator described creates a baseline for the future development of a complete digital model of the real satellite on-orbit. The modular structure of the software could be widened and made general, creating an adaptable tool to support mission analysis and design.

Acknowledgements

The research presented in this paper has been funded by Genergo.

References

[1] W. Yang, Y. Zheng and S. Li, "Application Status and Prospect of Digital Twin for On-Orbit Spacecraft," in *IEEE Access*, vol. 9, pp. 106489-106500, 2021, doi: 10.1109/ACCESS.2021.3100683.

[2] H. Yin Z, L. Wang, Application and Development Prospect of Digital Twin Technology in Aerospace, IFAC-PapersOnLine, Volume 53, Issue 5, 2020, pp. 732-737.

[3] O. Montenbruck, E. Gill, Force Model - Geopotential, in Satellite Orbits, Springer Berlin, Heidelberg, 2000, pp. 56-68.

[4] D. A. Vallado, Disturbing forces, in: Fundamentals of astrodynamics and applications, Microcosm Press, Hawthorne, 2013, pp. 538-590.

[5] T.S. Kelso, EOP and space weather data, 24 August 2022, https://celestrak.org/SpaceData/, (last accessed August 2022).

[6] D. A. Vallado, Celestial phenomena, in: Fundamentals of astrodynamics and applications, Microcosm Press and Springer, Hawthorne, 2013, pp. 277-316.

[7] F. L. Markley, J. L. Crassidis, External torques, in: Fundamentals of Spacecraft Attitude Determination and Control, Microcosm Press and Springer, New York, 2014, pp. 103-111.

[8] P. Fortescue, G. Swinerd, J. Stark, Spacecraft Systems Engineering, John Wiley & Sons Inc, 2014, Figure 4.15.